The adenoviral E1B-55k protein present in HEK293 cells mediates abnormal accumulation of key WNT signaling proteins in large cytoplasmic aggregates.

Petter Angell Olsen[1,2]* and Stefan Krauss[1,2]

1 Hybrid Technology Hub - Centre of Excellence, Institute of Basic Medical Sciences, University of Oslo, Oslo, Norway

2 Unit for Cell Signaling, Department of Immunology and Transfusion Medicine, Oslo University Hospital, Oslo, Norway.

*Correspondence: peteraol@medisin.uio.no

SUMMARY

HEK293 cells are one of the most widely used cell lines in research and HEK293 cells are frequently used as an *in vitro* model for studying the WNT signaling pathway. The HEK293 cell line was originally established by transfection of human embryonic kidney cells with sheared adenovirus 5 DNA and it is known that that HEK293 cells stably express the adenoviral E1A and E1B-55k proteins. Here we show that HEK293 cells display an unexpected distribution of key components of the WNT/β-catenin signaling pathway where AXIN1, APC, DVL2 and tankyrase are all co-localized in large spherical cytoplasmic aggregates. The cytoplasmic aggregates are enclosed by a narrow layer of the adenoviral E1B-55k protein. Reduction of E1B-55k protein levels leads to disappearance of the cytoplasmic aggregates thus corroborating an essential role of the E1B-55k protein in mediating the formation of the aggregates. Furthermore, HEK293 cells with reduced E1B-55k protein levels display reduced levels of transcriptional activation of WNT/β-catenin signaling upon stimulation by the Wnt3A agonist. The demonstrated influence of the E1B-55k protein on the cellular localization of WNT/β-catenin signaling components and on WNT/β-catenin signaling activity asks for caution in the interpretation of data derived from the HEK293 cell line.

INTRODUCTION

The WNT/β-catenin signaling pathway plays a pivotal role during development, organogenesis, stem cell maintenance and self-renewal of many tissues, and aberrant WNT/β-catenin signaling activity is associated with the development of several disease conditions including cancer (Clevers and Nusse, 2012; MacDonald et al., 2009). The main determinant of WNT/β-catenin signaling activity is the level of free cytoplasmic β-catenin that can translocate to the nucleus and activate target genes through interactions of β-catenin with transcription factors of the TCF/LEF family (Valenta et al., 2012). In cells with low WNT/β-catenin signaling activity, the levels of cytoplasmic β-catenin is kept low by the constant action of a degradosome that targets cytosolic β-catenin (by phosphorylation and ubiquitination) for proteolytic degradation. The degradosome comprises in its core the structural protein APC, the rate limiting structural proteins AXIN1/2, β-catenin, the kinases CK1 and GSK3β and the ubiquitin ligase β-TrCP (Stamos and Weis, 2013). A further protein, tankyrase (TNKS), may associate with the degradosome and regulate its activity by controlling the stability of the AXIN1/2 proteins (Haikarainen et al., 2014; Kamal et al., 2014). Activation of WNT/β-catenin signaling by binding of an exogenous WNT ligand, such as WNT3A, to the frizzled (Fz) and low-density lipoprotein receptor-related protein (LRP5/6) receptors at the cell membrane leads to interference with degradosome activity thus resulting in increased levels of cytosolic β-catenin (DeBruine et al., 2017). The typical model for degradosome inactivation upon WNT ligand receptor binding involves disassembly of the degradosome and formation of a signalosome due to interactions between AXIN1/2 and DVL2 at activated Fz and LRP5/6 membrane receptors (Gammons et al., 2016; Schwarz-Romond et al., 2007).

Cell lines are important tools in cell biology research and one of the most commonly used cell lines is human embryonic kidney (HEK) 293 cells (Graham et al., 1977; Lin et al., 2014). The HEK293 cell line was originally established by transfection of primary human embryonic kidney cells with sheared adenovirus 5 DNA and it has been shown that HEK293 cells stably express the adenoviral E1A and E1B-55k proteins due to integration of a 4 kbp adenoviral DNA fragment in chromosome 19 (Graham *et al.*, 1977; Louis et al., 1997). In the context of WNT/β-catenin signaling, HEK293 cells are frequently used as a model system since they do not contain known mutations in central WNT/β-catenin signaling components and have a functional WNT/β-catenin signaling cascade from the cell surface to the nucleus. Thus, HEK293 cells display low levels of basal canonical WNT/β-catenin signaling activity that efficiently can be

stimulated with exogenous WNT ligands, such as WNT3A, leading to increased transcription of WNT/β-catenin target genes (Gujral and MacBeath, 2010; Jia et al., 2008; Li et al., 2012).

Given the broad use of HEK293 cells in WNT signaling research, we have characterized the subcellular localization of key components of the WNT/β-catenin signaling pathway. We show that while β-catenin is predominantly localized at the cell membrane, AXIN1, APC, DVL2 and TNKS all co-localize in large cytoplasmic aggregates that are enclosed by a narrow layer of the adenoviral E1B-55k protein present in HEK293 cells. We further analyzed E1B-55k protein interaction partners and identify the AMER1 protein as a potential link between WNT signaling components and the E1B-55k protein in HEK293 cells. Finally, we demonstrate that siRNA mediated reduction of E1B-55k protein levels lead to a dispersal of the cytoplasmic bodies and that HEK293 cells with reduced E1B-55k protein levels display reduced WNT/β-catenin transcriptional activation upon stimulation with Wnt3A.

RESULTS AND DISCUSSION

Key WNT signaling components are localized in large cytoplasmic aggregates in HEK293 cells

To characterize the subcellular localization of central WNT/β-catenin signaling components, immunofluorescence (IF) staining was performed on untreated HEK293 cells and on cells incubated either with Wnt3A conditioned medium (CM) to activate the WNT signaling pathway, or with the TNKS inhibitor G007-LK to inhibit WNT signaling activity (due to stabilization of the degradosome (Lau et al., 2013; Lehtio et al., 2013; Voronkov and Krauss, 2013)). IF staining of β-catenin confirmed its established localization pattern: In untreated HEK293 cells, the majority of β-catenin was predominantly located at the cell membranes (Fig. 1, row I, left column). Treatment of cells with Wnt3A CM resulted in increased levels of β-catenin both in the cytoplasm and in the nucleus (Fig. 1, row I middle column). In cells treated with G007-LK the localization of β-catenin was unchanged relative to what was observed in untreated cells (Figure 1, row I, right column). Interestingly, IF staining of AXIN1, APC and DVL2 displayed an accumulation of these proteins in large cytoplasmic aggregates that also contained TNKS (Figure 1, rows II, III and IV). Typically, each cell contained only one of these large cytoplasmic perinuclear aggregates. We were not able to detect AXIN2 in HEK293 cells

by IF (not shown) which probably reflects the low expression levels of AXIN2 (2.9 – 4.8 transcripts-per million (Malm et al., 2020; Thul et al., 2017)). Treatment of cells with either Wnt3A or G007-LK did not influence the cytoplasmic localization or amount of APC or DVL2 (Figure 1, row III and IV, middle columns). However, both AXIN1 and TNKS displayed increased fluorescent staining intensity following G007-LK treatment thus demonstrating G007-LK mediated stabilization of AXIN1 and TNKS protein levels (Figure 1, right columns) as previously observed (Huang et al., 2009; Waaler et al., 2012).

The cytoplasmic aggregates are organized in spherical structures enclosed by a narrow layer of the adenoviral E1B-55k protein, which is required for aggregate formation.

The sub-cellular localization and size of β-catenin degradosomes have been reported to vary between experimental systems and cell lines (Stamos and Weis, 2013). However, the accumulation of central WNT/β-catenin signaling components in a single large cytoplasmic body as observed in the HEK293 cell line has not been described in other cell lines. The HEK293 cell line was originally established by transfection with sheared adenoviral DNA and it has been shown that these cells express the adenoviral E1A and E1B proteins (Graham *et al.*, 1977; Louis *et al.*, 1997). It has further been demonstrated in E1A and E1B transformed cell lines that, while E1A displays a nuclear localization, the E1B-55k protein commonly localizes in large cytoplasmic aggregates (Brown et al., 1994; Horwitz et al., 2008; Madison et al., 2002; Zantema et al., 1985). To investigate if the observed cytoplasmic aggregates in HEK293 cells co-localized with the E1B-55k protein, IF staining of the two proteins was performed. As seen in Figure 2 the majority of E1B-55k protein accumulated in large cytoplasmic aggregates that co-localized with the TNKS stained cytoplasmic bodies. Although small clusters of E1B-55k that did not co-localize with TNKS were also present, all TNKS positive bodies displayed co-localization with the large E1B-55k protein aggregates.

To investigate a possible role of the E1B-55k protein in the formation of the cytoplasmic aggregates and to gain insight into the protein organization in the TNKS/E1B-55k aggregates, siRNA was used to reduce E1B-55k protein levels and structured illumination microscopy (SIM) (Gustafsson, 2000) was used to acquire high resolution images. SIM imaging of E1B-55k and TNKS proteins in HEK293 cells treated with control siRNA revealed that the cytoplasmic TNKS aggregates were assembled in spheroid structures composed of a central

TNKS core encapsulated by a narrow layer of E1B-55k protein (Figure 3A) (hereafter referred to E1B-55k aggregates). In Supplementary Movie M1 an animated three-dimensional rendering of a TNKS stained aggregate enclosed with the E1B-55k protein layer is shown. The E1B-55k aggregates varied in size with diameters ranging from 1 to 4 μm (not shown) and the width of the E1B-55k protein layer surrounding TNKS was measured to be around 230 nm (Figure S1). Treatment of HEK293 cells with two independent E1B-55k siRNAs efficiently reduced the E1B-55k protein levels to 29 % and 18 % 72 hours after transfection (Figure S2). E1B-55k siRNA treatment led to a disappearance of the spherical TNKS aggregates in the majority of cells (Figure 3B) thus reducing of the average number of TNKS aggregates per cell from 0.75 to 0.18 (Figure 3C). Some E1B-55k protein could still be detected in E1B-55k siRNA treated cells however, rather than enclosing TNKS in spherical arrangements, the remaining E1B-55k protein formed rod like structures (Figure 3B). The TNKS protein displayed a uniform cytoplasmic localization in the E1B-55k siRNA treated cells, although some of the TNKS protein co-localized with the remaining E1B-55k in the rod like structures (Figure 3B). Similar to TNKS the cellular distribution of AXIN1, APC and DVL2 was changed from accumulation in the E1B-55k aggregates to a uniform cytoplasmic distribution in the E1B-55k siRNA treated cells (Figure S3). These results establish that the E1B-55k protein was mediating the formation and accumulation of central WNT/β-catenin components in large cytoplasmic aggregates in HEK293 cells.

Analysis of E1B-55k interaction partners in HEK293 cells

To identify E1B-55k interaction partners in HEK293 cells and to identify possible links between the E1B-55k protein and components of the WNT/β-catenin signaling pathway, co-immunoprecipitation (Co-IP) was carried out. Total cell HEK293 cell extracts were immune-precipitated (IP) with anti E1B-55k antibodies and proteins present in the immunoprecipitates were identified by liquid chromatography-tandem mass spectrometry (LS-MS/MS) in two independent experiments (Table 1). The list of proteins that were detected in both experiments included previously well-established E1B-55k interaction partners such as TP53 and components of the MRN DNA repair complex (MRE11, RAD50 and NBN)(Hidalgo et al., 2019; Hung and Flint, 2017). An interaction of E1B-55k with TP53, as detected in the IP of HEK293 cells, has been shown in several cellular systems and sequestration of TP53 in E1B-55k clusters and is seen as a way for adenoviruses to neutralize TP53 activation during infection (Blackford and Grand, 2009; Zhao and Liao, 2003). Although not well established, interactions

between TP53 and the WNT signaling components AXIN1, DVL2 and GSK3β have been reported (Li et al., 2011; Rual et al., 2005; Rui et al., 2004; Vinayagam et al., 2011; Watcharasit et al., 2002; Yachie et al., 2016). Further possible direct links between E15-55k and WNT/β-catenin signaling pathway components included the APC and AMER1 proteins that were detected as E1B-55k interaction partners in one of the Co-IP experiments. APC is large multifunctional protein with scaffolding functional that is essential for assembly of the β-catenin destruction complex (Nelson and Nathke, 2013). An association between APC and E1B-55k would be compatible with the observed clustering of key WNT signaling components in the E1B-55k aggregates nevertheless, APC has not been detected as an E1B-55k interaction partner previously. On the other hand, AMER1 (also called WTX) has been shown to interact both with the β-catenin destruction complex (Grohmann et al., 2007; Major et al., 2007) and the E1B-55k protein (Kim et al., 2012). AMER1 regulates WNT signaling activity through its role as a scaffold protein for the β-catenin destruction complex (Tanneberger et al., 2011) and would accordingly represents a feasible candidate protein mediating sequestering of WNT signaling components in the E1B-55k clusters. Though, a conclusive identification of the link between the E1B-55k protein and key components of the WNT signaling pathway will require validation by additional experiments that is outside the scope of this work.

Reduction of E1B-55k protein levels in HEK293 cells cause decreased WNT/β-catenin mediated transcriptional activation upon Wnt3A agonist treatment.

Given the observed E1B-55k mediated accumulation of TNKS, AXIN1, APC and DVL2 in cytoplasmic aggregates (Figure 3 and Figure S3) we next examined the impact of the cytoplasmic E1B-55k aggregates on WNT/β-catenin signaling activation. First, protein levels of TNKS, AXIN1 and DVL2 were analyzed after E1B-55k siRNA treatment and as seen in Figure 4A, E1B-55k knock down did not influence on the total protein levels of TNKS, AXIN1 or DVL2. Next, the impact of E1B-55k siRNA treatment on β-catenin dependent transcriptional activation was tested using a SuperTopFlash (STF) reporter cell line (Veeman et al., 2003). The HEK293-STF/Ren cell line incorporates a stably integrated β-catenin responsive STF Firefly luciferase reporter together with a constitutive active control Renilla luciferase reporter and represents a robust assay for quantifying changes in WNT/β-catenin signaling (Voronkov et al., 2013). When control siRNA transfected HEK293-STF/Ren cells were incubated with increasing amounts (0-2-10-30 %) of Wnt3A CM, the STF reporter was activated in a dose dependent manner reaching a maximum 23 fold induction compared to untreated cells (Figure

4B). HEK-STF/Ren cells transfected with E1B-55k siRNA also displayed a dose dependent activation of STF by Wnt3A CM, however, in these cells the level of STF activation reached a maximum 12 fold induction with 30 % Wnt3A. The observed increased potency of WNT/β-catenin signaling activation in HEK293 cells with native E1B-55k protein levels would be compatible with a scenario where the aggregation of central components of the β-catenin destruction complex in the E1B-55k clusters interferes with the destruction complex activity.

In this work we have shown that in HEK293 cells central components of the WNT/β-catenin signaling pathway are sequestered in the cytoplasmic E1B-55k aggregates that influence the functional activity of the β-catenin destruction complex. By super-resolution microscopy, we have established that the aggregates have a spherical structure that is surrounded by a narrow layer of E1B-55k protein. Formation of these aggregates depends on the presence of E1B-55k protein and HEK293 cells with reduced E1B-55k protein levels displays reduced WNT/β-catenin mediated transcriptional activation. The established effect of E1B-55k on both the cytoplasmic localization of components of the WNT/β-catenin pathway and on the activity of WNT/β-catenin signaling in HEK293 cells asks for caution in the interpretation of data derived from this standard WNT signaling "work horse" cell line.

LIMITATIONS OF THE STUDY

Although the Co-IP experiments performed identified candidate proteins that could mediate the association of key WNT signaling components in the E1B-55k aggregates, further experiments is required to identify and verify the underlying proteins and mechanisms.

ACKNOWLEDGMENTS

We thank P. Branton for providing the E1B-55k antibody and M. Melheim for technical assistance. We acknowledge the financial support of the Research Council of Norway grant number 262613 and the Norwegian Cancer Society grant number 4561000.

AUTHOR CONTRIBUTIONS

Conceptualization, P.A.O and S.K.; Methodology, Investigations, Visualization and Writing - original draft, P.A.O; Writing – Review & Editing, P.A.O and S.K.; Funding Acquisition and Supervision, S.K.

DECLARATION OF INTERESTS

The authors declare no competing interests.

SUPPLEMENTAL INFORMATION

Figure S1. Measurement of E1B-55k protein layer thickness.

Figure S3. In HEK293 cells with reduced E1B-55k protein levels the distribution of AXIN1, APC and DVL2 is changed from accumulation in aggregates to a more uniform cytoplasmic distribution.

Table S1 and S2. E1B-55k interacting partners detected in Co-IP experiment 1 and 2.

Movie S1. 3D rendering of a TNKS stained aggregate enclosed with the E1B-55k protein layer.

Table 1. E1B-55k interacting partners detected by Co-IP

Experiment 1	Experiment 2	Identified in both experiments
RAD50	*RAD50*	*RAD50*
MRE11	*USP9X*	*USP9X*
USP9X	*MRE11*	*MRE11*
TP53	*TP53*	*TP53*
SDCCAG3	*PRRC2B*	*PRRC2B*
KRT78	*PHLDB2*	*PHLDB2*
PRRC2B	*NBN*	*NBN*
ATAD3A	SNX9	*HADHA*
PHLDB2	YTHDC2	*WAPL*
ARG1	*HADHA*	*TRIM27*
NBN	APC	*SDCCAG3*
TGM3	RAB11FIP2	*BAG2*
CASP14	*WAPL*	*IRS4*
MEIOC	DSG1	*LAMB3*
TNRC6A	TCOF1	*TNRC6A*
BAG2	*TRIM27*	*CUL9*
ZNF318	*SDCCAG3*	*ZNF318*
PRC1	*BAG2*	*CASP14*
TNRC6B	*IRS4*	*MYO1B*
TRAF7	TCF25	*MEIOC*
LAMB3	*LAMB3*	*ERH*
LMO7	TRIM28	
CUL7	CLASP1	
AZGP1	*TNRC6A*	
ERH	HAL	
KPRP	PKP4	
MYO1B	ZSWIM8	
AKAP8	*CUL9*	
ENO1	*ZNF318*	
GGCT	COIL	
CEP131	SNX33	
POF1B	FYCO1	
CORO1C	WASHC2A	
TRIM27	PCM1	
HNRNPF	GTF3C3	
CALML5	AGTPBP1	
KRT6C	TNRC6C	
DSC3	LAMA3	
GIGYF1	AGRN	
CUL9	LAMB1	
MYO1C	*CASP14*	
MYH10	RPS24	
ALOX12B	RPL4	
HADHA	SBSN	
SERPINB12	ITIH2	
AUNIP	VTN	
LIMA1	*MYO1B*	
WAPL	FLNA	
FLG	CARD10	
DLC1	*MEIOC*	
KIF14	SLC25A11	
DDX17	AMER1	
EIF4E2	TJP2	
UNC13C	BAIAP2L1	
IRS4	ZSCAN20	
BCLAF1	FAM83B	
IGHG4	SBNO1	
	AHDC1	
	RPL35	
	ERH	

Proteins in experiment 1 and 2 are sorted according to their "Mascot Score". Proteins detected in both experiments are in italic and previously identified E1B-55k interacting proteins are underlined. Further details can be found in Supplementary Table 1 and 2.

FIGURE LEGENDS

Figure 1. Key WNT/β-catenin signaling components localizes in large cytoplasmic aggregates in HEK293 cells.

Representative fluorescent images (laser wide field (WF)) of untreated, Wnt3A and G007-LK treated HEK293 cells immunostained for β-catenin, TNKS, AXIN1, APC and DVL2 as indicated. Single channel and merged images are shown. In the merged color images, nuclear counterstaining is shown in blue. Scale bar: 10 μM.

Figure 2. The adenoviral E1B-55k protein present in HEK293 cells co-localize with the large cytoplasmic aggregates

IF analysis (laser WF) of the localization of the E1B-55k and TNKS proteins in untreated HEK293 cells. In the merged color image E1B-55k and TNKS co-localization is indicated with arrows and nuclear counterstaining is shown in blue. Scale bar: 10 μM.

Figure 3. The cytoplasmic aggregates is organized in a spherical structure which is enclosed by a narrow layer of adenoviral E1B-55k protein and reduction of E1B-55k protein levels causes disassembly of the spherical aggregates.

Representative SIM images of HEK293 cells treated with (A) control or (B) E1B-55k siRNA. Upper rows displays single channel images of E1B-55k and TNKS as indicated with scale bar representing 10 μm. In the merged color images nuclear counterstaining is shown in blue. The scale bar represents 10 μm. Enlargements of the stippled boxes in the merged image are show to the right (single Z plane) with scale bars representing 1 μm. (C) Quantification of mean number of cytoplasmic spherical aggregates per cell in control and E1B-55k siRNA treated cells. Each point represent the mean number of cytoplasmic aggregates per cell in one microscopic view field. For each siRNA treatment 10 random view fields were quantified. The red asterisk indicate significant difference between control and E1B-55k siRNA treated cells ($P<0001$).

Figure 4. Reduction of E1B-55k protein levels in HEK293 cells cause decreased WNT/β-catenin mediated transcriptional activation upon Wnt3A agonist treatment.

(A) Western blot analysis of E1B-55k, TNKS, AXIN1 and DVL2 protein levels in untreated (-) and HEK293 cells treated with E1B-55k and control siRNA as indicated. Actin protein levels as loading control are shown below the corresponding bands. (B) STF reporter gene assay measuring β-catenin mediated transcriptional activation in HEK293-STF/Ren cells treated with none (-), control or two independent E1B-55k siRNA constructs (I and II). The cells were incubated in growth medium supplemented with 0, 2, 10 or 30 % Wnt3A CM as indicated. Shown is fold STF activation relative to untreated cells (without siRNA and Wnt3A CM) from three parallel measurements and error bars represent SD. Asterisk indicate significant difference relative to control siRNA treated cells (grown in 30 % Wnt3A CM); E1B-55k siRNA (I) P=0.0016, E1B-55k siRNA (II) P=0003.

METHODS

Cell lines

The human embryonic kidney cell lines HEK293 (ATCC CRL-1573) and HEK293T (ATCC CRL-3216) was obtained from the American Type Culture Collection (Manassas, VA, USA). The stable reporter HEK-STF/Ren cell line have been described previously (Voronkov *et al.*, 2013). All cell lines were cultured in DMEM (Thermo Fisher Scientific) supplemented with 10 % FBS and 1 % penicillin/streptomycin (Merck) at 37°C in a humidified atmosphere containing 5 % CO_2.

Manipulation of WNT signaling activity by Wnt3A CM and G007-LK treatment

To stimulate or inhibit WNT signaling activity cells were treated for 24 hours with Wnt3A CM or G007-LK, respectively. Wnt3A CM was prepared by collecting the supernatant from L Wnt3A cells (ATCC CRL-2647) according to the manufactures protocol. Unless otherwise stated, HEK293 cells were treated with Wnt3A CM diluted 50 % in complete DMEM. Stock solutions of G007-LK (Voronkov *et al.*, 2013) was prepared in DMSO and was added to the growth medium at a final concentration of 1 µM.

Immunofluorescence staining and microscopy

Cells grown on coverslips pre-coated with poly-L-lysine (Merck) were fixed in 4 % paraformaldehyde (15 minutes at room temperature (RT) permeabilized with 0.1 % Triton-X100/PBS (15 minutes at RT) followed by incubation with primary and secondary antibodies diluted in PBS with 4 % bovine serum albumin (1 hour RT each). Nuclear counterstaining was performed with DAPI (1 µg/ml, 5 minutes RT) and the coverslips were mounted in ProLong Diamond Antifade Mountant (Thermo Fisher Scientific). The following primary antibodies and dilutions were used: β-catenin (BD Biosciences; BD610153; 1:500), Tankyrase-1/2 (H-350) (Santa Cruz Biotechnology; sc-8337; 1:50), Tankyrase-1/2 (E10) (Santa Cruz Biotechnology; sc-365897; 1:40), AXIN1 (C76H11) (Cell Signalling Technology; #2087; 1:50), APC (F-3) (Santa Cruz Biotechnology; sc-9998; 1:50), DVL2 (10B5) (Santa Cruz Biotechnology; sc-8026; 1:50), E1B-55k (2A6) (Generous gift from P.E. Branton (Querido et al., 2001); 1:50), SV40 T Antigen (Ab-2) (Merck Millipore; DP02; 5 µg/ml). Secondary antibodies (all from Thermo Fisher Scientific; 1:500): anti-Rabbit IgG Alexa488 (A-21206), anti-Mouse IgG

Alexa488 (A-11001), anti-Rabbit IgG Alexa594 (A-11012), anti-Mouse IgG Alexa594 (A-11005), anti-Rabbit IgG Alexa647 (A-21246), anti-Mouse IgG Alexa647 (A-31571). Fluorescent images were acquired with a Zeiss Elyra PS1 microscope system using standard filters sets and laser lines with a Plan-APOCHROMAT 63x 1.4 NA oil objective. Images were acquired using the "Laser wide field (WF)" or "Structured Illumination Microscopy (SIM)" mode of the system as indicated. SIM images are specified in the figure legends. Laser WF images were acquired for 30 Z planes and are displayed as maximum intensity projections rendered from all Z planes. SIM images were acquired using 5 grid rotations with the 0.51 µm grid for 22 Z planes with a Z spacing of 0.184 nm between planes. SIM images were reconstructed with the following "Method" parameters in the ZEN black software (Carl Zeiss Micro Imaging): Processing: manual; Noise Filter: -5.5; SR Frequency Weighting: 1; Baseline Cut; Sectioning: 100/83/83; Output: SR-SIM; PSF: Theoretical. Unless otherwise mentioned SIM images are displayed as maximum intensity projections rendered from all Z planes.

Co-immunoprecipitation (Co-IP)

Total HEK293 cell lysates was prepared by lysing cells in ice-cold lysis buffer (50 mM Tris pH 7.5, 150 mM NaCl, 1.5 mM $MgCl_2$, 0.5 % Nonidet P-40, and cOmplete Protease Inhibitor Cocktail (Roche)) for 20 minutes on ice. For Co-IP, Dynabeads protein G (Thermo Fisher Scientific) was used according to the manufacturer's instructions. Briefly, antibodies (control normal mouse IgG (Santa Cruz Biotechnology; 2 ug) and (E1B-55k; 10 µl)) were bound to 50 µl washed beads by incubation for 1 hour at room temperature. The antibody coated beads were then incubated with cell lysate (400 µg total protein) at 4 ^{o}C overnight. The beads with immune complexes were washed four times with lysis buffer and two times with PBS/0.02 % Tween-20 and resuspended in PBS before analysis by liquid chromatography-tandem mass spectrometry (LS-MS/MS).

LS-MS/MS analysis

Beads from the Co-IP were dissolved in 20 µL 0.2 % ProteaseMAX™ Surfactant, Trypsin Enhancer (Promega) in 50 mM NH_4HCO_3 followed by protein reduction, alkylation and on-beads digestion with trypsin (Promega) overnight in 37 °C. After digestion, the samples were centrifuged at 14 000 x g for 10 min, trypsin was inactivated by adding 100 µl 1 % TFA, and

the samples were again centrifuged at 14 000 x g for 10 min. The resulting peptides were desalted and concentrated before mass spectrometry by the STAGE-TIP method using a C18 resin disk (3M Empore). Each peptide mixture was analyzed by a nEASY-LC coupled to QExactive Plus (ThermoElectron, Bremen, Germany) with EASY Spray PepMap®RSLC column (C18, 2 µl, 100Å, 75 µm x 50 cm). The resulting MS raw files were submitted for protein identification using Proteome Discoverer 2.1 (Thermo Fisher Scientific) and Mascot 2.5 (MatrixScience) search engine. The search criteria for Mascot searches were: trypsin digestion with two missed cleavage allowed, Carbamidomethyl (C) as fixed modification and Acetyl (N-term), Gln->pyro-Glu (N-term Q), Oxidation (M) as dynamic modifications. The parent mass tolerance was 10 ppm and MS/MS tolerance 0.1 Da. The SwissProt database was used for the database searches. All of the reported protein identifications were statistically significant ($p<0.05$) in Mascot and filtered in ProteomeDiscoverer for at least medium confidence identifications.

siRNA transfection

Cells were transfected with the indicated siRNA construct (40 nM final concentration) using the Lipofectamine 2000 transfection reagent (Thermo Fisher Scientific) according to the manufacturer's instructions. The transfection mixture was kept on the cells for 24 hours followed by growth medium replacement and incubation for another 48 hours before fixation for immunofluorescence or preparation of cell lysates for western blot analysis. The following siRNA sequences were used: Control siRNA: endoribonuclease-prepared siRNA pool (esiRNA) that that target multiple locations in the EGFP mRNA sequence (Merck; EHUEGFP), E1B-55k siRNA (I): (GGA GCG AAG AAA CCC AUC UGA UU) and E1B-55k siRNA (II): (GGC CAG AUU GCA AGU ACA AGA UU). E1B-55k siRNA constructs I and II targets nucleotide positions 3-23 and 542-562 in the E1B-55k CDS, respectively (from HAdV5 GenBank accession no. AY339865.1: 2019-3509).

Quantification of spherical TNKS bodies number in cells

Quantification of average number of spherical TNKS bodies per cell was done by counting number of spherical TNKS bodies per cell per cell in 10 randomly acquired images from control and E1B-55k siRNA treated cells (>100 cells counted per treatment).

Western blot analysis

Total cell lysates were prepared by lysing cells ice cold RIPA buffer (Thermo Fisher Scientific) supplemented with cOmplete Protease Inhibitor Cocktail (Roche) for 20 minutes on ice. Protein concentrations were quantified by the Pierce BCA Protein Assay kit (Thermo Fisher Scientific). Lysates (20 µg total protein) were electrophoresed (NuPAGE Novex 3-8 % Tris-Acetate Protein Gels (Thermo Fisher Scientific)) and transferred to PVDF membranes (Immobilon-P (Merck Millipore)). Immunodetection of proteins were done by incubation with primary antibodies overnight at 4° C and incubation with secondary antibodies for 1 hour at room temperature. The following primary antibodies and dilutions were used: Tankyrase-1/2 (E10) (Santa Cruz Biotechnology; sc-365897; 1:200), AXIN1 (C76H11) (Cell Signalling Technology; #2087; 1:1000), DVL22 (30D2) (Cell Signalling Technology; #3224; 1:1000), E1B-55k (2A6) (Generous gift from P.E. Branton (Querido *et al.*, 2001); 1:5000), β-catenin (BD Biosciences; BD610153; 1:5000), actin (Merck, A2066, 1:4000). Secondary antibodies (all from Santa Cruz Biotechnology; 1:5000): chicken anti-rabbit IgG-HRP (sc-2955), chicken anti-mouse IgG-HRP (sc-2954). Chemiluminescent detection was performed with the ECL Prime Western Blotting Detection Reagent (Amersham – GE Healthcare Life sciences) and the ChemiDoc Touch Imaging System (Bio-Rad).

Supertop flash (STF) luciferase reporter gene assay

Analysis of the effect of the E1B-55k protein on WNT signaling was performed using the HEK293-STF/ren cell line where the β-catenin responsive TCF/LEF driven reporter (7xTCF/LEF binding sites regulating firefly luciferase expression) and the constitutive CMV Renilla luciferase constructs are stably integrated (Voronkov *et al.*, 2013). One day after plating in 6 well dishes HEK293-STF/Ren cells were left untreated or transfected with control or E1B-55k siRNA. 24 hours after siRNA transfection the cells were splitted, distributed in 12 well dishes and incubated for 24 hours before the growth medium was replaced with medium containing increasing amounts (0, 2, 10 and 30 %) of Wnt3A conditioned media (CM). After 24 hours incubation with Wnt3A CM the cells were harvested in passive lysis buffer and both firefly and Renilla luciferase activity was measured in the same sample using the Dual-Luciferase Reporter Assay System (Promega). The luminescence was quantified on a GloMax-Multi microplate reader (Promega) according to the manufacturer's instructions. For figure preparation the ratios of firefly luciferase to Renilla luciferase signals were used. Wnt3A CM

was prepared from L Wnt3A-expressing cells (ATCC CRL-2647) according to the manufacturer's instructions.

Statistical analysis

Calculation of statistical significant difference between means was done using the two sample unpaired t-test.

REFERENCES

Blackford, A.N., and Grand, R.J. (2009). Adenovirus E1B 55-kilodalton protein: multiple roles in viral infection and cell transformation. J Virol *83*, 4000-4012. 10.1128/JVI.02417-08.

Brown, C.R., Doxsey, S.J., White, E., and Welch, W.J. (1994). Both viral (adenovirus E1B) and cellular (hsp 70, p53) components interact with centrosomes. J Cell Physiol *160*, 47-60. 10.1002/jcp.1041600107.

Clevers, H., and Nusse, R. (2012). Wnt/beta-catenin signaling and disease. Cell *149*, 1192-1205. 10.1016/j.cell.2012.05.012.

DeBruine, Z.J., Xu, H.E., and Melcher, K. (2017). Assembly and architecture of the Wnt/beta-catenin signalosome at the membrane. Br J Pharmacol *174*, 4564-4574. 10.1111/bph.14048.

Gammons, M.V., Renko, M., Johnson, C.M., Rutherford, T.J., and Bienz, M. (2016). Wnt Signalosome Assembly by DEP Domain Swapping of Dishevelled. Mol Cell *64*, 92-104. 10.1016/j.molcel.2016.08.026.

Graham, F.L., Smiley, J., Russell, W.C., and Nairn, R. (1977). Characteristics of a human cell line transformed by DNA from human adenovirus type 5. J Gen Virol *36*, 59-74. 10.1099/0022-1317-36-1-59.

Grohmann, A., Tanneberger, K., Alzner, A., Schneikert, J., and Behrens, J. (2007). AMER1 regulates the distribution of the tumor suppressor APC between microtubules and the plasma membrane. J Cell Sci *120*, 3738-3747. 10.1242/jcs.011320.

Gujral, T.S., and MacBeath, G. (2010). A system-wide investigation of the dynamics of Wnt signaling reveals novel phases of transcriptional regulation. PLoS One *5*, e10024. 10.1371/journal.pone.0010024.

Gustafsson, M.G. (2000). Surpassing the lateral resolution limit by a factor of two using structured illumination microscopy. J Microsc *198*, 82-87. 10.1046/j.1365-2818.2000.00710.x.

Haikarainen, T., Krauss, S., and Lehtio, L. (2014). Tankyrases: structure, function and therapeutic implications in cancer. Curr Pharm Des *20*, 6472-6488. 10.2174/1381612820666140630101525.

Hidalgo, P., Ip, W.H., Dobner, T., and Gonzalez, R.A. (2019). The biology of the adenovirus E1B 55K protein. FEBS Lett *593*, 3504-3517. 10.1002/1873-3468.13694.

Horwitz, G.A., Zhang, K., McBrian, M.A., Grunstein, M., Kurdistani, S.K., and Berk, A.J. (2008). Adenovirus small e1a alters global patterns of histone modification. Science *321*, 1084-1085. 10.1126/science.1155544.

Huang, S.M., Mishina, Y.M., Liu, S., Cheung, A., Stegmeier, F., Michaud, G.A., Charlat, O., Wiellette, E., Zhang, Y., Wiessner, S., et al. (2009). Tankyrase inhibition stabilizes axin and antagonizes Wnt signalling. Nature *461*, 614-620. 10.1038/nature08356.

Hung, G., and Flint, S.J. (2017). Normal human cell proteins that interact with the adenovirus type 5 E1B 55kDa protein. Virology *504*, 12-24. 10.1016/j.virol.2017.01.013.

Jia, L., Miao, C., Cao, Y., and Duan, E.K. (2008). Effects of Wnt proteins on cell proliferation and apoptosis in HEK293 cells. Cell Biol Int *32*, 807-813. 10.1016/j.cellbi.2008.03.011.

Kamal, A., Riyaz, S., Srivastava, A.K., and Rahim, A. (2014). Tankyrase inhibitors as therapeutic targets for cancer. Curr Top Med Chem *14*, 1967-1976. 10.2174/1568026614666140929115831.

Kim, W.J., Rivera, M.N., Coffman, E.J., and Haber, D.A. (2012). The WTX tumor suppressor enhances p53 acetylation by CBP/p300. Mol Cell *45*, 587-597. 10.1016/j.molcel.2011.12.025.

Lau, T., Chan, E., Callow, M., Waaler, J., Boggs, J., Blake, R.A., Magnuson, S., Sambrone, A., Schutten, M., Firestein, R., et al. (2013). A Novel Tankyrase Small-molecule Inhibitor Suppresses APC Mutation-driven Colorectal Tumor Growth. Cancer Res.

Lehtio, L., Chi, N.W., and Krauss, S. (2013). Tankyrases as drug targets. FEBS J *280*, 3576-3593. 10.1111/febs.12320.

Li, Q., He, Y., Wei, L., Wu, X., Wu, D., Lin, S., Wang, Z., Ye, Z., and Lin, S.C. (2011). AXIN is an essential co-activator for the promyelocytic leukemia protein in p53 activation. Oncogene *30*, 1194-1204. 10.1038/onc.2010.499.

Li, V.S., Ng, S.S., Boersema, P.J., Low, T.Y., Karthaus, W.R., Gerlach, J.P., Mohammed, S., Heck, A.J., Maurice, M.M., Mahmoudi, T., et al. (2012). Wnt signaling through inhibition of beta-catenin degradation in an intact Axin1 complex. Cell *149*, 1245-1256. 10.1016/j.cell.2012.05.002.

Lin, Y.C., Boone, M., Meuris, L., Lemmens, I., Van Roy, N., Soete, A., Reumers, J., Moisse, M., Plaisance, S., Drmanac, R., et al. (2014). Genome dynamics of the human embryonic kidney 293 lineage in response to cell biology manipulations. Nat Commun *5*, 4767. 10.1038/ncomms5767.

Louis, N., Evelegh, C., and Graham, F.L. (1997). Cloning and sequencing of the cellular-viral junctions from the human adenovirus type 5 transformed 293 cell line. Virology *233*, 423-429. 10.1006/viro.1997.8597.

MacDonald, B.T., Tamai, K., and He, X. (2009). Wnt/beta-catenin signaling: components, mechanisms, and diseases. Dev Cell *17*, 9-26. 10.1016/j.devcel.2009.06.016.

Madison, D.L., Yaciuk, P., Kwok, R.P., and Lundblad, J.R. (2002). Acetylation of the adenovirus-transforming protein E1A determines nuclear localization by disrupting association with importin-alpha. J Biol Chem *277*, 38755-38763. 10.1074/jbc.M207512200.

Major, M.B., Camp, N.D., Berndt, J.D., Yi, X., Goldenberg, S.J., Hubbert, C., Biechele, T.L., Gingras, A.C., Zheng, N., Maccoss, M.J., et al. (2007). Wilms tumor suppressor WTX negatively regulates WNT/beta-catenin signaling. Science *316*, 1043-1046. 10.1126/science/1141515.

Malm, M., Saghaleyni, R., Lundqvist, M., Giudici, M., Chotteau, V., Field, R., Varley, P.G., Hatton, D., Grassi, L., Svensson, T., et al. (2020). Evolution from adherent to suspension: systems biology of HEK293 cell line development. Sci Rep *10*, 18996. 10.1038/s41598-020-76137-8.

Nelson, S., and Nathke, I.S. (2013). Interactions and functions of the adenomatous polyposis coli (APC) protein at a glance. J Cell Sci *126*, 873-877. 10.1242/jcs.100479.

Querido, E., Blanchette, P., Yan, Q., Kamura, T., Morrison, M., Boivin, D., Kaelin, W.G., Conaway, R.C., Conaway, J.W., and Branton, P.E. (2001). Degradation of p53 by adenovirus E4orf6 and E1B55K proteins occurs via a novel mechanism involving a Cullin-containing complex. Genes Dev *15*, 3104-3117. 10.1101/gad.926401.

Rual, J.F., Venkatesan, K., Hao, T., Hirozane-Kishikawa, T., Dricot, A., Li, N., Berriz, G.F., Gibbons, F.D., Dreze, M., Ayivi-Guedehoussou, N., et al. (2005). Towards a proteome-scale map of the human protein-protein interaction network. Nature *437*, 1173-1178. 10.1038/nature04209.

Rui, Y., Xu, Z., Lin, S., Li, Q., Rui, H., Luo, W., Zhou, H.M., Cheung, P.Y., Wu, Z., Ye, Z., et al. (2004). Axin stimulates p53 functions by activation of HIPK2 kinase through multimeric complex formation. EMBO J *23*, 4583-4594. 10.1038/sj.emboj.7600475.

Schwarz-Romond, T., Fiedler, M., Shibata, N., Butler, P.J., Kikuchi, A., Higuchi, Y., and Bienz, M. (2007). The DIX domain of Dishevelled confers Wnt signaling by dynamic polymerization. Nat Struct Mol Biol *14*, 484-492. 10.1038/nsmb1247.

Stamos, J.L., and Weis, W.I. (2013). The beta-catenin destruction complex. Cold Spring Harb Perspect Biol *5*, a007898. 10.1101/cshperspect.a007898.

Tanneberger, K., Pfister, A.S., Kriz, V., Bryja, V., Schambony, A., and Behrens, J. (2011). Structural and functional characterization of the Wnt inhibitor APC membrane recruitment 1 (Amer1). J Biol Chem *286*, 19204-19214. 10.1074/jbc.M111.224881.

Thul, P.J., Akesson, L., Wiking, M., Mahdessian, D., Geladaki, A., Ait Blal, H., Alm, T., Asplund, A., Bjork, L., Breckels, L.M., et al. (2017). A subcellular map of the human proteome. Science *356*. 10.1126/science.aal3321.

Valenta, T., Hausmann, G., and Basler, K. (2012). The many faces and functions of beta-catenin. EMBO J *31*, 2714-2736. 10.1038/emboj.2012.150.

Veeman, M.T., Slusarski, D.C., Kaykas, A., Louie, S.H., and Moon, R.T. (2003). Zebrafish prickle, a modulator of noncanonical Wnt/Fz signaling, regulates gastrulation movements. Curr Biol *13*, 680-685. 10.1016/s0960-9822(03)00240-9.

Vinayagam, A., Stelzl, U., Foulle, R., Plassmann, S., Zenkner, M., Timm, J., Assmus, H.E., Andrade-Navarro, M.A., and Wanker, E.E. (2011). A directed protein interaction network for investigating intracellular signal transduction. Sci Signal *4*, rs8. 10.1126/scisignal.2001699.

Voronkov, A., Holsworth, D.D., Waaler, J., Wilson, S.R., Ekblad, B., Perdreau-Dahl, H., Dinh, H., Drewes, G., Hopf, C., Morth, J.P., et al. (2013). Structural basis and SAR for G007-LK, a lead stage 1,2,4-triazole based specific tankyrase 1/2 inhibitor. J Med Chem *56*, 3012-3023. 10.1021/jm4000566.

Voronkov, A., and Krauss, S. (2013). Wnt/beta-catenin signaling and small molecule inhibitors. Curr.Pharm.Des *19*, 634-664.

Waaler, J., Machon, O., Tumova, L., Dinh, H., Korinek, V., Wilson, S.R., Paulsen, J.E., Pedersen, N.M., Eide, T.J., Machonova, O., et al. (2012). A novel tankyrase inhibitor decreases canonical Wnt signaling in colon carcinoma cells and reduces tumor growth in conditional APC mutant mice. Cancer Res *72*, 2822-2832. 10.1158/0008-5472.CAN-11-3336.

Watcharasit, P., Bijur, G.N., Zmijewski, J.W., Song, L., Zmijewska, A., Chen, X., Johnson, G.V., and Jope, R.S. (2002). Direct, activating interaction between glycogen synthase kinase-3beta and p53 after DNA damage. Proc Natl Acad Sci U S A *99*, 7951-7955. 10.1073/pnas.122062299.

Yachie, N., Petsalaki, E., Mellor, J.C., Weile, J., Jacob, Y., Verby, M., Ozturk, S.B., Li, S., Cote, A.G., Mosca, R., et al. (2016). Pooled-matrix protein interaction screens using Barcode Fusion Genetics. Mol Syst Biol *12*, 863. 10.15252/msb.20156660.

Zantema, A., Fransen, J.A., Davis-Olivier, A., Ramaekers, F.C., Vooijs, G.P., DeLeys, B., and Van der Eb, A.J. (1985). Localization of the E1B proteins of adenovirus 5 in transformed cells, as revealed by interaction with monoclonal antibodies. Virology *142*, 44-58. 10.1016/0042-6822(85)90421-0.

Zhao, L.Y., and Liao, D. (2003). Sequestration of p53 in the cytoplasm by adenovirus type 12 E1B 55-kilodalton oncoprotein is required for inhibition of p53-mediated apoptosis. J Virol *77*, 13171-13181. 10.1128/jvi.77.24.13171-13181.2003.

Figure 1

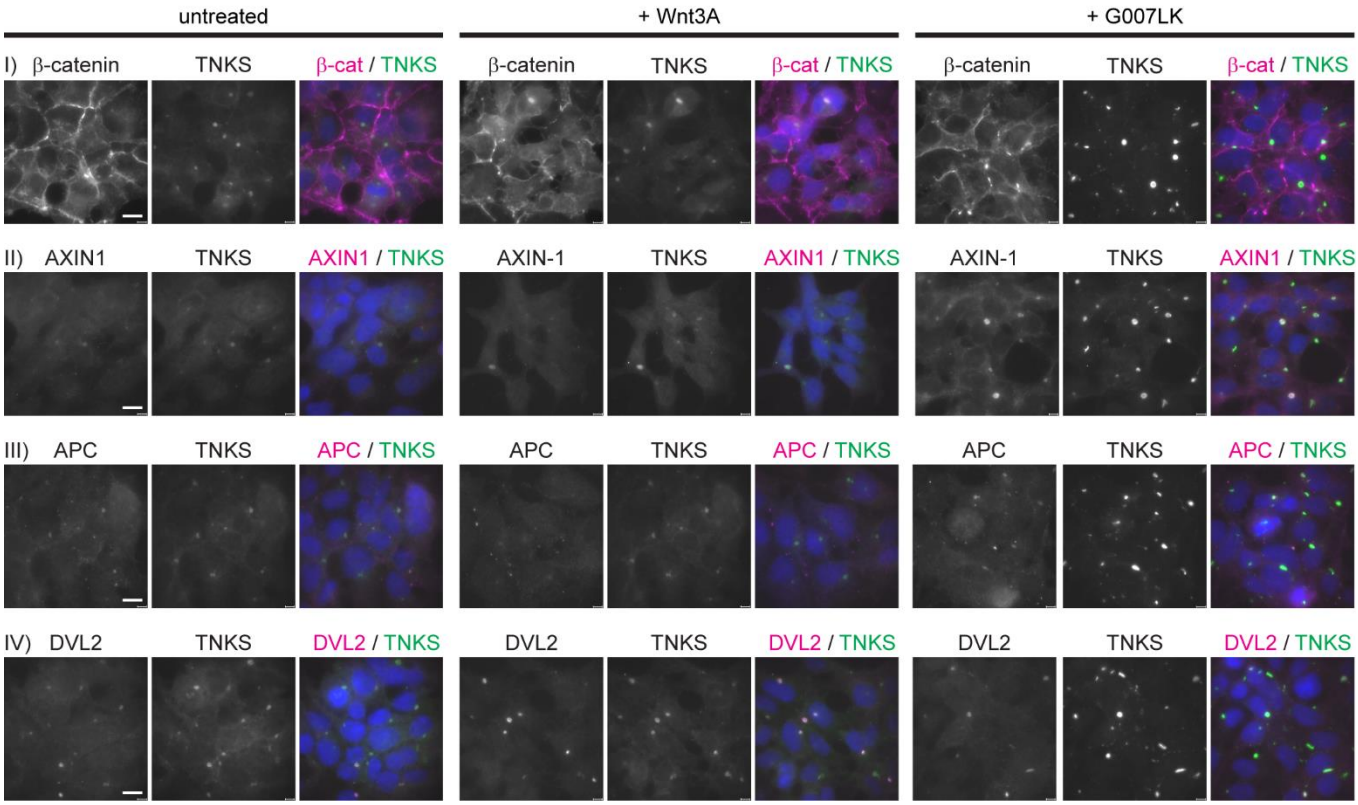

Figure 2

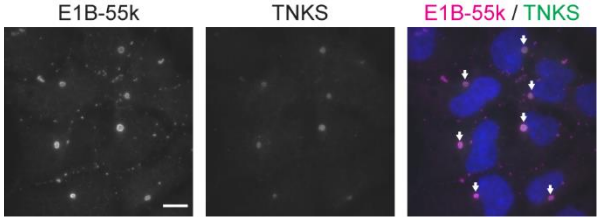

Figure 3

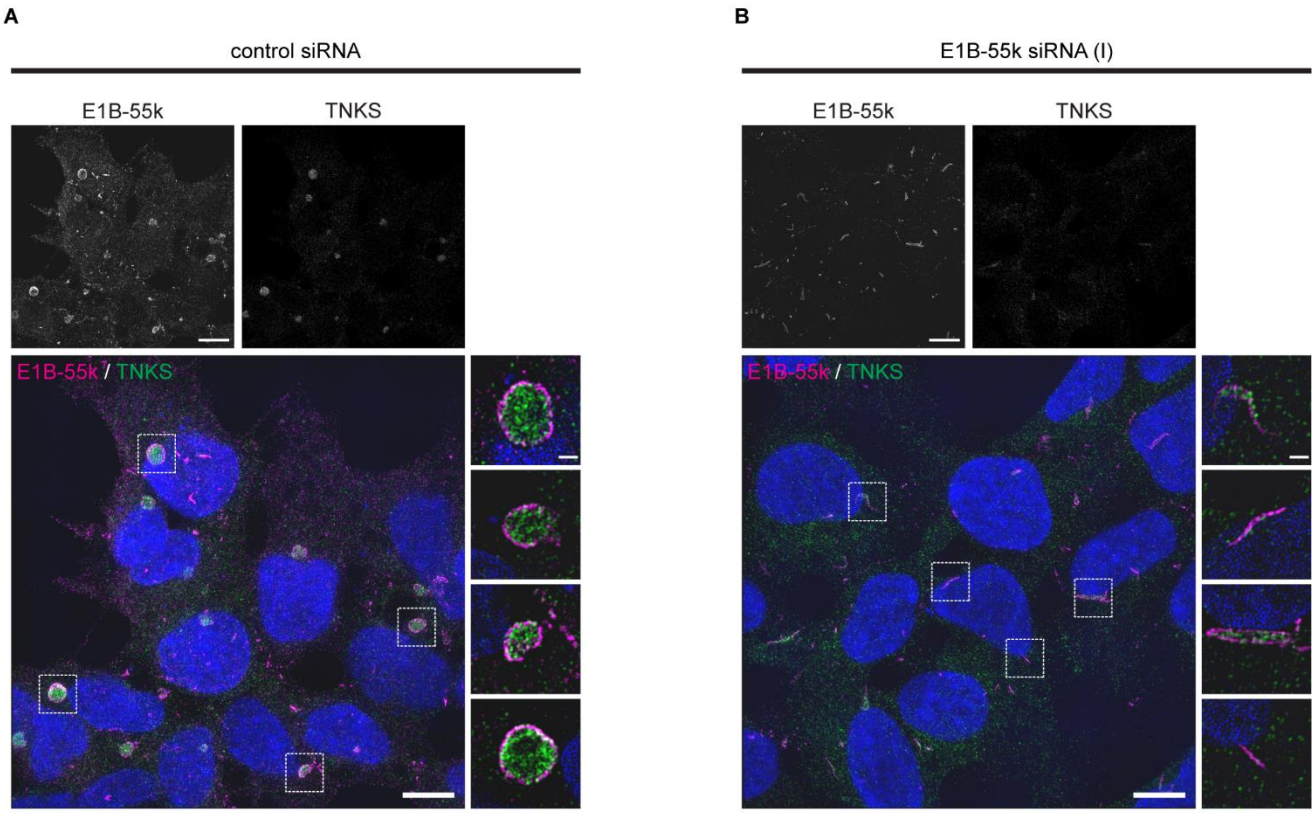
A
control siRNA
E1B-55k
TNKS
E1B-55k / TNKS
B
E1B-55k siRNA (I)
E1B-55k
TNKS
E1B-55k / TNKS

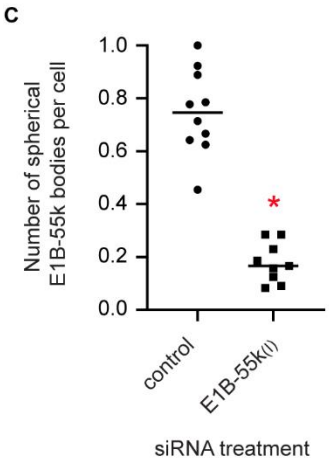
C
Number of spherical E1B-55k bodies per cell
1.0
0.8
0.6
0.4
0.2
0.0
*
control
E1B-55k(I)
siRNA treatment

Figure 4

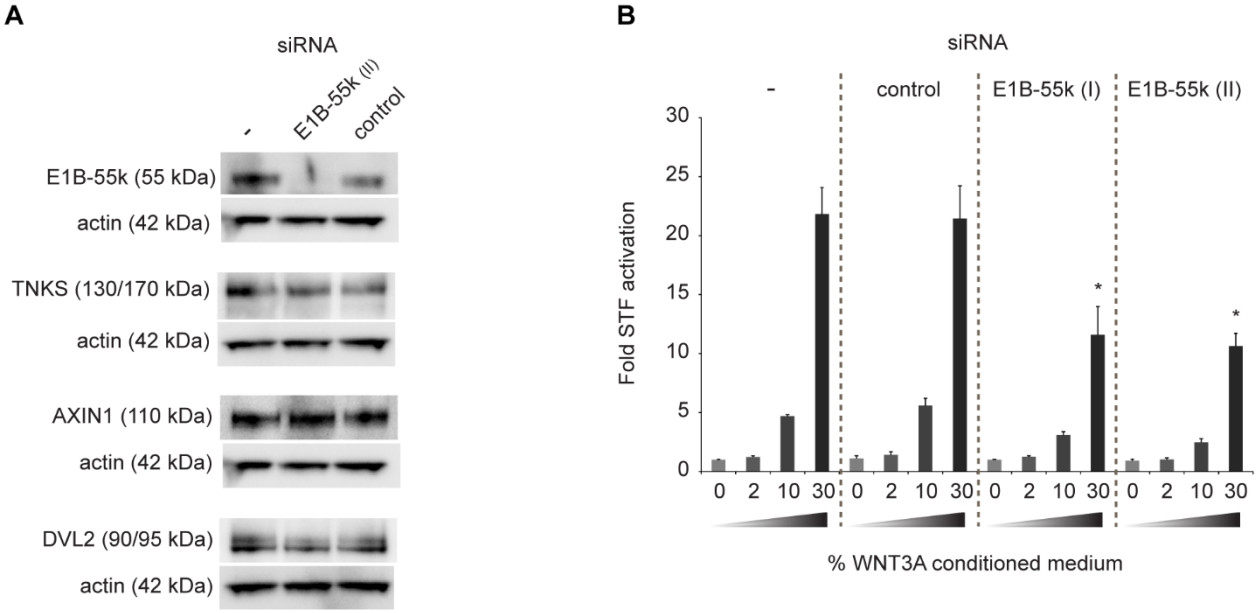
A
siRNA
-
E1B-55k (II)
control
E1B-55k (55 kDa)
actin (42 kDa)
TNKS (130/170 kDa)
actin (42 kDa)
AXIN1 (110 kDa)
actin (42 kDa)
DVL2 (90/95 kDa)
actin (42 kDa)
B
siRNA
-
control
E1B-55k (I)
E1B-55k (II)
Fold STF activation
30
25
20
15
10
5
0
0 2 10 30 0 2 10 30 0 2 10 30 0 2 10 30
% WNT3A conditioned medium